The authors in [1] appear to assume that $r(\gamma_i^2 I_n - \Gamma) = n - m_i$ for all $i = 1, \cdots, k$. A correct development for distinct eigenvalues is given, i.e., $k = n$ (although they only show the solution for a line of infinite length). They appear to assume that the fully degenerate case ($k=1$) is given by Amemiya in [7]. However, Amemiya assumes $\boldsymbol{R} = \boldsymbol{G} = {}_n0_n$ and also that $\boldsymbol{CL} = (1/v_0^2) I_n$. This therefore insures that although all eigenvalues are the same, ($\gamma_i^2 = 1/v_0^2$), $r[\gamma_i^2 I_n - p^2 \boldsymbol{CL}] = 0$ and $\boldsymbol{\Gamma}$ is already in diagonal Jordan form. This would correspond to n lossless conductors imbedded in a lossless homogeneous medium [8]. One of the main results of [1, eq. (10)] seems to be in error. The modal matrix in [1, eq. (10)], $[\alpha]$ (whose columns obviously must be eigenvectors of $\boldsymbol{ZY}$), is shown for $s = n - m$ equal eigenvalues with the remaining m eigenvalues distinct.

Since [1, eq. (7)] must be a solution to [1, eq. (1c)], it seems clear that the structure of $[\alpha]$ given in [1, eq. (10)] is only valid if $\boldsymbol{ZY}$ is partially diagonal (since $[V_{ii}]$ in [1] is diagonal) as

$$\boldsymbol{ZY} = \left[\begin{array}{c|c} & {}_m0_s \\ K & \text{-----} \\ & K^* \end{array}\right] \tag{16}$$

where $\boldsymbol{K}$ is $n \times m$ and $\boldsymbol{K}^*$ is an $s \times s$ diagonal matrix with identical scalar elements γ^{2*} on the main diagonal. This, of course, is a special case of all possible structures of $\boldsymbol{ZY}$.

There do exist certain practical cases where diagonalization of $\boldsymbol{\Gamma}$ can be shown *a priori*. If we neglect loss, i.e., $\boldsymbol{G} = \boldsymbol{R} = {}_n0_n$, and assume $\boldsymbol{C}$ symmetric and positive definite and $\boldsymbol{L}$ symmetric, then one may determine a real nonsingular transformation matrix $\boldsymbol{T}$ such that $\boldsymbol{T}^{-1}\boldsymbol{\Gamma}\boldsymbol{T} = p^2 \boldsymbol{T}^{-1}\boldsymbol{CLT}$ is diagonal. This is an application of the simultaneous diagonalization of two quadratic forms [10]. The assumption of $\boldsymbol{C}$ and $\boldsymbol{L}$ being symmetric is in most cases quite acceptable and $\boldsymbol{C}$ will be positive definite if (1) is written so that

$$[C_{ii}] = C_{iG} + \sum_{\substack{j=1 \\ j \neq i}}^{n} C_{ij} \quad \text{and} \quad [C_{ij}] = -C_{ij} \;\; j \neq i$$

where we denote the element of $\boldsymbol{C}$ in the ith row and jth column by $[C_{ij}]$, C_{iG} is the capacitance of the ith conductor to ground, and C_{ij} is the mutual capacitance between conductor i and conductor j. Subroutine NROOT in the IBM scientific subroutine package performs this type of reduction. Then the change of variables $I(x) = \boldsymbol{T} I_m(x)$ will "decouple" (3) with $\boldsymbol{T}^{-1} = \boldsymbol{T}^T \boldsymbol{C}^{-1}$, where we denote the transpose of a matrix $\boldsymbol{T}$ by $\boldsymbol{T}^T$.

It is also possible to include losses if we assume $\boldsymbol{R} = r(p) I_n$ (identical conductors), $\boldsymbol{G} = {}_n0_n$, $\boldsymbol{CL} = 1/v_0^2 \; I_n$, and $\boldsymbol{C}$ is symmetric, and positive definite. Then $\boldsymbol{\Gamma} = pr(p)\boldsymbol{C} + p^2/v_0^2 I_n$. The transformation $I(x) = \boldsymbol{T} I_m(x)$ such that $\boldsymbol{T}^{-1}\boldsymbol{CT}$ is diagonal will decouple (3) and the existence of $\boldsymbol{T}$ is guaranteed since $\boldsymbol{C}$ is real, symmetric.

Finally, there exist certain cyclic symmetric matrices for which diagonalization of $\boldsymbol{\Gamma}$ does not depend upon the entries in $\boldsymbol{Z}$ and $\boldsymbol{Y}$. For example, if $n=3$ $[Z_{ii}] = Z$, $[Z_{12}] = [Z_{23}] = [Z_{31}] = Z'$, $[Z_{13}] = [Z_{21}] = [Z_{32}] = Z''$, and $\boldsymbol{Y}$ has a similar structure, then there exists a simple coordinate transformation $\boldsymbol{T}$ with $[T_{1j}] = [T_{i1}] = 1/\sqrt{3}$ for $i, j = 1, 2, 3$ $[T_{22}] = [T_{33}] = a^2/\sqrt{3}$, and $[T_{23}] = [T_{32}] = a/\sqrt{3}$ with $a = e^{j2\pi/3}$ and $\boldsymbol{T}^{-1} = \boldsymbol{T}^*$, where * denotes complex-conjugate transpose which will diagonalize $\boldsymbol{\Gamma}$. This is sometimes referred to as a symmetrical coordinate transformation and can be extended for $n > 3$ [12]. This technique would apply to n wires within a conducting cylinder arranged symmetrically about the axis.

If $r(\gamma_i^2 I_n - \boldsymbol{\Gamma}) = n - m_i$, for all $i = 1, \cdots, k$, then a set of n linearly independent eigenvectors $\boldsymbol{T}_{ij}$, for $j = 1, \cdots, m_i$, may be found satisfying

$$(\gamma_i^2 I_n - \boldsymbol{\Gamma}) \boldsymbol{T}_{ij} = {}_n0_1 \tag{17}$$

where $\boldsymbol{T}_{ij}$ is an $n \times 1$ vector function of p which is also a column of $\boldsymbol{T}$. If $r(\gamma_i^2 I_n - \boldsymbol{T}) > n - m_i$ for some repeated root γ_i^2, then one may find generalized eigenvectors which place $\boldsymbol{\Gamma}$ in Jordan canonical form [4]. For sinusoidal excitations ($p = j\omega$), machine computation of eigenvectors is straightforward, although tedious if all n eigenvalues of $\boldsymbol{\Gamma}$ are not distinct.

References

[1] H. Guckel and Y. Y. Sun, "Uniform multimode transmission lines," *IEEE Trans. Microwave Theory Tech.* (Short Paper), vol. MTT-20, pp. 412–413, June 1972.
[2] W. Kaplan, *Ordinary Differential Equations.* Reading, Mass.: Addison-Wesley, 1958.
[3] F. R. Gantmacher, *The Theory of Matrices.* New York: Chelsea, 1960.
[4] K. Ogata, *State Space Analysis of Control Systems.* Englewood Cliffs, N. J.: Prentice-Hall, 1967.
[5] C. R. Paul and Y. L. Kuo, "Controllability and observability of multivariable systems," *IEEE Trans. Automat. Contr.* (Corresp.), vol. AC-16, pp. 207–209, Apr. 1971.
[6] R. C. Peirson and E. C. Bertnolli, "A novel method for solving the uniform distributed network analysis problem," *Proc. IEEE* (Lett.), pp. 2169–2170, Dec. 1968.
[7] H. Amemiya, "Time-domain analysis of multiple parallel transmission lines," *RCA Rev.*, vol. 28, pp. 241–276, 1967.
[8] L. V. Bewley, *Traveling Waves on Transmission Systems.* New York: Dover, 1963.
[9] S. O. Rice, "Steady state solutions of transmission line equations," *Bell Syst. Tech. J.*, vol. XX, no. 2, pp. 131–178, Apr. 1941.
[10] S. Perlis, *Theory of Matrices.* Reading, Mass.: Addison-Wesley, 1952.
[11] L. A. Pipes, "Direct computation of transmission matrices of electrical transmission lines: Part I," *J. Franklin Inst.*, vol. 281, no. 4, pp. 275–292, Apr. 1966.
[12] S. Hayashi, *Surges on Transmission Systems.* Kyoto, Japan: Denki-Shoin, 1955.

On the Surface-to-Bulk Mode Conversion of Rayleigh Waves

CHI-PIN CHANG AND HANG-SHENG TUAN

***Abstract*—The surface-to-bulk wave conversion phenomena occurring at a discontinuity characterized by a surface contour deformation may be used as a means for tapping Rayleigh waves in a nonpiezoelectric solid. For this purpose, the mode conversion problem is treated in this short paper with the use of a boundary perturbation technique. A systematic procedure is obtained to calculate not only the first-order scattered waves which include the reflected surface wave and the converted bulk wave, but also the higher order terms. With careful design of the surface contour, the converted bulk-wave power and the direction of propagation into the substrate may be controlled.**

I. Introduction

Surface acoustic waves have received considerable attention in recent years [1], [2]. One important application of surface waves is in signal processing devices [3]–[5], where their use can reduce device length by several orders of magnitude compared with their electromagnetic counterparts. Hence, an integration of acoustic devices with integrated electronics is promising. One important factor which has put these devices into practical use is the introduction of interdigital transducers [6], [7] which have high efficiency in exciting, receiving, and tapping acoustic surface waves. However, interdigital transducers only operate on the surface of a piezoelectric crystal. For devices requiring longer delay length and more taps, larger crystals are needed, which are difficult to grow.

If a nonpiezoelectric solid is used for the main delay path in connection with a piezoelectric substrate [8]–[10], there will be no length problem, but acoustic surface waves should be tapped along the main path by methods other than interdigital fingers. In a previous paper [11], we have studied a discontinuity problem in the hope that we may use the surface-to-bulk wave transduction at a guiding discontinuity for tapping Love waves. In this short paper, we treat a similar problem for the case of Rayleigh waves. The geometry is shown in Fig. 1. For $z \leq 0$, it is a semi-infinite nonpiezoeelectric elastic medium with density ρ and Lame's elastic constants λ_e and μ, where λ is reserved to denote the Rayleigh wavelength. The guiding surface $z=0$ has a region of deformation around $x=0$ shown by the dotted line, while the solid line indicates a perfect surface. Consider a Rayleigh wave incident from left to right along the x axis. A bulk wave will be generated due to the discontinuity. It propagates into the substrate with certain directional characteristics which depend on the exact geometrical shape of the deformation. This bulk wave may be detected in the bottom of the substrate if the directional property of the beam is known. By the use of the boundary perturbation technique [12], [13], the mode conversion problem is systematically analyzed.

Manuscript received September 11, 1972, revised November 20, 1972. This work was supported by NASA under Grant NGL 33-015-066.
C. P. Chang was with the Department of Electrical Sciences, State University of New York, Stony Brook, N. Y. 11790. He is now with ACCO, Bristol Datamaster Division, Glen Cove, N. Y.
H. S. Tuan is with the Department of Electrical Sciences, State University of New York, Stony Brook, N. Y. 11790.

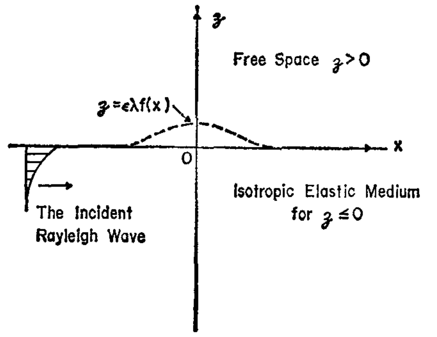

Fig. 1. Geometry of the problem.

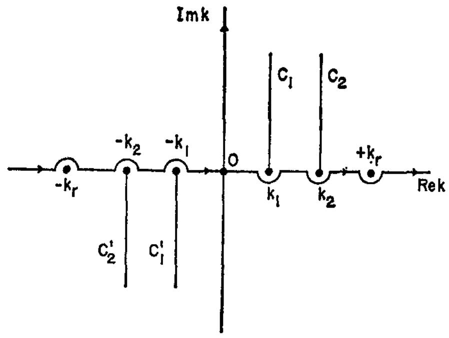

Fig. 2. The integration path in k plane.

II. The Incident Rayleigh Wave

The particle displacement u_i of the incident wave may be derived from a scalar potential ϕ_i and a vector potential $\hat{y}\psi_i$, namely, $u_i = \nabla\phi_i + \nabla\times\hat{y}\psi_i$. With the harmonic time dependence $e^{-i\omega t}$, it may be shown that ϕ_i and ψ_i satisfy the following wave equations:

$$\left(\frac{\partial^2}{\partial x^2}+\frac{\partial^2}{\partial z^2}+k_1^2\right)\phi_i = 0, \quad \left(\frac{\partial^2}{\partial x^2}+\frac{\partial^2}{\partial z^2}+k_2^2\right)\psi_i = 0 \tag{1}$$

where

$$k_1 = \frac{\omega}{v_1}, \quad k_2 = \frac{\omega}{v_2}, \quad v_1 = \sqrt{\frac{\lambda_e + 2\mu}{\rho}}, \quad \text{and} \quad v_2 = \sqrt{\frac{\mu}{\rho}}.$$

For the incident Rayleigh wave, ϕ_i and ψ_i are given by

$$\phi_i = \frac{1}{2ik_r\sqrt{k_r^2 - k_1^2}}\, e^{ik_r x} e^{\sqrt{k_r^2-k_2^2}\, z}$$

$$\psi_i = \frac{1}{2k_r^2 - k_2^2}\, e^{ik_r x} e^{\sqrt{k_r^2-k_2^2}\, z} \tag{2}$$

where the wavenumber k_r satisfies

$$-4k^2\sqrt{k_r^2 - k_1^2}\sqrt{k_r^2 - k_2^2} + (2k_r^2 - k_2^2)^2 = 0. \tag{3}$$

III. Excitation of Rayleigh Waves by a Line Source—The Green's Functions

Consider a line source located at $z=0$ and $x=x'$. The Green's functions ϕ_G and ψ_G, which are the elastic potential functions, satisfy the equations in (1), respectively. The line source simultaneously applies tangential and normal stresses at $x=x'$ which are

$$T_{zx}|_{z=0} = -P(x')\delta(x-x') \quad \text{and} \quad T_{zz}|_{z=0} = -Q(x')\delta(x-x') \tag{4}$$

where $P(x')$ and $Q(x')$ denote the two amplitudes of stresses at x'. The two Green's functions may be given by

$$\phi_G(x, z; x', z'=0) = \frac{-1}{2\pi\mu}\int_{-\infty}^{\infty} \frac{2k\xi_2 P + (2k^2 - k_2^2)Q}{F(k)}\, e^{ik(x-x')}e^{-i\xi_1 z}\, dk \tag{5}$$

$$\psi_G(x, z; x', z'=0) = \frac{1}{2\pi\mu}\int_{-\infty}^{\infty} \frac{(2k^2 - k_2^2)P - 2k\xi_1 Q}{F(k)}\, e^{ik(x-x')}e^{-i\xi_2 z}\, dk \tag{6}$$

where $F(k) = 4k^2\xi_1\xi_2 + (2k^2 - k_2^2)^2$

$$\begin{aligned}\xi_1 &= \sqrt{k_1^2 - k^2}, & |k| &< k_1\\ &= i\sqrt{k^2 - k_1^2}, & |k| &> k_1\\ \xi_2 &= \sqrt{k_2^2 - k^2}, & |k| &< k_2\\ &= i\sqrt{k^2 - k_2^2} & |k| &> k_2.\end{aligned} \tag{7}$$

The path of integration for (5) and (6) is along the real axis of the complex k plane. The evaluation of (5) and (6) by the contour integration technique necessitates the introduction of appropriate branch cuts and indentations around poles. The result is given in Fig. 2. It may be shown that, for $F(k)=0$, the pair of real roots occurring at $\pm k_r$ is identical to the propagation constants of Rayleigh waves. Clearly, the residue contributions of the poles at $\pm k_r$ to (5) and (6) give Rayleigh waves propagating in the $\pm x$ directions along the surface $z=0$. Moreover, (5) and (6) contain bulk waves which propagate into the substrate.

IV. Boundary Perturbation Formulation

The main problem of this short paper is formulated in this section. As shown in Fig. 1, the deformed surface is defined by the function $S \equiv S(x, z) = z - \lambda\epsilon f(x) = 0$, where λ is the Rayleigh wavelength and ϵ is a small real number such that $|\lambda\epsilon f'(x)|$ is less than one in the region where $df(x)/dx$ is a continuous function. Since the incident Rayleigh wave does not satisfy the elastic boundary conditions on the deformed surface, we introduce the complete solution to the problem as follows:

$$\phi = \phi_i + \sum_{m=1}^{\infty}\epsilon^m\phi_m \quad \text{and} \quad \psi = \psi_i + \sum_{m=1}^{\infty}\epsilon^m\psi_m. \tag{8}$$

Then, ϕ and ψ must satisfy (1). Because ϵ is just a small parameter, we conclude that each pair, ϕ_m and ψ_m which may be called the mth-order scattered field, should satisfy (1) also. The boundary conditions for solving (8) are the tangential and normal stresses to vanish on S. These conditions may be cast in the following forms:

$$\left.\begin{aligned} T_{nn} &= \mu\left[2\frac{\partial^2}{\partial t\partial n}\phi + \left(\frac{2}{\partial t^2} - \frac{\partial^2}{\partial n^2}\right)\psi\right] = 0\\ T_{nt} &= \left[\lambda_e\frac{\partial^2}{\partial t^2} + (\lambda_e + 2\mu)\frac{\partial^2}{\partial n^2}\right]\phi + 2\mu\frac{\partial^2}{\partial n\partial t}\psi = 0\end{aligned}\right\}\ \text{on } S \tag{9}$$

where the subscripts n and t indicate the normal and tangential directions on S. It may be shown that

$$\frac{\partial}{\partial n} = (\hat{n}\cdot\nabla) = \frac{1}{\sqrt{1+\left(\lambda\epsilon\frac{df}{dx}\right)^2}}\left(\frac{\partial}{\partial z} - \lambda\epsilon\frac{df}{dx}\frac{\partial}{\partial x}\right)$$

$$\frac{\partial}{\partial t} = (\hat{t}\cdot\nabla) = \frac{1}{\sqrt{1+\left(\lambda\epsilon\frac{df}{dx}\right)^2}}\left(\lambda\epsilon\frac{df}{dx}\frac{\partial}{\partial z} + \frac{\partial}{dx}\right). \tag{10}$$

Substituting (10) into (9), we get a set of boundary conditions which are combinations of $\partial/\partial x$ and $\partial/\partial z$ operating on ϕ and ψ equating to zero on S. Expanding the results in Taylor series about the unperturbed boundary $z=0$ for small ϵ, requiring that each pair of the coefficient functions for a different power of ϵ be zero, we may obtain the boundary conditions for solving each order of the scattered fields. The first two-pair coefficient functions so obtained are given as follows:

$$\epsilon^0;\quad L_1(\phi_i, \psi_i) = 0 \quad \text{and} \quad L_2(\phi_i, \psi_i) = 0, \qquad \text{at } z = 0 \tag{11}$$

where

$$L_1(\phi_i, \psi_i) \equiv 2\mu\frac{2}{\partial x\partial z}\phi_i + \mu\left(\frac{\partial^2}{\partial x^2} - \frac{\partial^2}{\partial z^2}\right)\psi_i$$

$$L_2(\phi_i, \psi_i) \equiv \left(\lambda_e\nabla^2 + 2\mu\frac{\partial^2}{\partial z^2}\right)\phi_i + 2\mu\frac{\partial^2}{\partial x\partial z}\psi_i$$

$$\begin{aligned}\epsilon^1;\quad & L_1(\phi_1, \psi_1) - 2\mu\lambda\frac{df}{dx}\left(\frac{\partial^2}{\partial x^2}\phi_i - \frac{\partial^2}{\partial z^2}\phi_i - 2\frac{\partial^2}{\partial x\partial z}\psi_i\right)\\ &+ \mu\lambda f(x)\left(2\frac{\partial^2}{\partial x\partial z}\phi_i - \frac{\partial^3}{\partial z^3}\psi_i + \frac{\partial^3}{\partial x^2\partial z}\psi_i\right) = 0, \qquad \text{at } z = 0\\ & L_2(\phi_1, \psi_1) + \lambda_e\lambda f(x)\left(\frac{\partial^3}{\partial x^2\partial z}\phi_i + \frac{\partial^3}{\partial z^3}\phi_i\right)\\ &+ 2\mu\lambda f(x)\left(\frac{\partial^3\phi_i}{\partial z^3} + \frac{\partial^3}{\partial x\partial z^2}\psi_i\right) = 0, \qquad \text{at } z = 0.\end{aligned} \tag{12}$$

Higher order terms may be also obtained in the same manner. It is clear that (11) gives the regular two boundary conditions for the incident Rayleigh wave, whereas (12) gives the needed boundary conditions for solving the first-order scattered fields ϕ_1 and ψ_1. We may rearrange (12) into the following convenient forms:

$$\begin{aligned} L_1(\phi_1, \psi_1) &= 2\mu\lambda \frac{df}{dx}\left(\frac{\partial^2}{\partial x^2}\phi_i - \frac{\partial^2}{\partial z^2}\phi_i - 2\frac{\partial^2}{\partial x \partial z}\psi_i\right) \\ &\quad - \mu\lambda f(x)\left(2\frac{\partial^3}{\partial x \partial z^2}\phi_i - \frac{\partial^3}{\partial z^3}\psi_i + \frac{\partial^3}{\partial x^2 \partial z}\psi_i\right) \\ &= -P_1(x), \qquad \text{at } z = 0 \\ L_2(\phi_1, \psi_1) &= -\lambda_e\lambda f(x)\left(\frac{\partial^3}{\partial x^2 \partial z}\phi_i + \frac{\partial^3}{\partial z^3}\phi_i\right) \\ &\quad - 2\mu\lambda f(x)\left(\frac{\partial^3}{\partial z^3}\phi_i + \frac{\partial^3}{\partial x \partial z^2}\psi_i\right) \\ &= -Q_1(x), \qquad \text{at } z = 0. \end{aligned} \tag{13}$$

It is seen that (13) represents stresses T_{zx} and T_{zz}, respectively, on the unperturbed surface $z=0$. These nonzero stresses are due to the interaction between the incident Rayleigh wave and the guiding surface deformation. Hence, (13) may be considered as a sheet of first-order line sources which generate the first-order scattered fields ϕ_1 and ψ_1. Similarly, we may obtain mth-order sources which will be in terms of the incident Rayleigh wave and lower order scattered fields up to $(m-1)$. The perturbation method used here is clearly a replacement of the original boundary condition on S by some induced distribution of sources on the unperturbed surface at $z=0$.

With the help of (5) and (6), the solution for ϕ_1 and ψ_1 may be written as

$$\phi_1(x, z) = \frac{-1}{2\pi\mu}\int_{-b}^{b}\int_{-\infty}^{\infty} \frac{+2k\xi_2 P_1(x') + (2k^2 - k_2^2)Q_1(x')}{F(k)} \cdot e^{ik(x-x')}e^{-i\xi_1 z}\, dk dx' \tag{14}$$

$$\psi_1(x, z) = \frac{1}{2\pi\mu}\int_{-b}^{b}\int_{-\infty}^{\infty} \frac{(2k^2 - k_2^2)P_1(x') - 2k\xi_1 Q_1(x')}{F(k)} \cdot e^{ik(x-x')}e^{-i\xi_2 z}\, dk dx' \tag{15}$$

where $P_1(x')$ and $Q_1(x')$ are given by (13) replacing x by x', and $-b$ to b is the range for which $f(x)$ exists. The path of integration is along the real axis of the complex k plane shown in Fig. 2. It is seen that the first-order scattered fields depend on the shape of the surface deformation through the dependence of variable x'. The second-order scattered fields are found as follows. Firstly, obtain the equivalent line source distribution $P_2(x')$ and $Q_2(x')$ from the third-pair coefficient functions of ϵ^2 in the Taylor series expansion. Then, $\phi_2(x, z)$ and $\psi_2(x, z)$ may be obtained with the repeated help of the Green's functions (5) and (6). Similarly, all other higher order scattered fields proposed in (8) may be found in the same manner.

V. Discussion and Conclusion

The evaluation of (14) and (15) may be carried out with the help of the contour integration technique. It can be shown that the reflected surface wave is due to the pole contribution at $k=-k_r$. The expression may be obtained quite easily. The bulk wave radiated into the substrate is contributed by two branch cut integrations along C_1 and C_2, shown in Fig. 2. The leading term for the far field may be obtained by the steepest descent integration technique. The details of these are omitted here, as similar calculations are given in (11). To design the discontinuity for purpose of tapping Rayleigh waves, we need to properly select the function $f(x)$ and the value of ϵ. As the bulk-wave power coupled out at the tap is proportional to ϵ^2, the direction of propagation depends on the exact geometric shape of the surface deformation. In an actual device, only a small portion of the incident power is used at each tap. Naturally, it requires a deformed surface contour with small ϵ value. Therefore, the perturbation formulation of this type of discontinuity is believed to give an approximate solution.

References

[1] *IEEE Trans. Microwave Theory Tech.* (*Special Issue on Microwave Acoustics*), vol. MTT-17, Nov. 1969.
[2] *Microwave J.* (*Special Issue on Microwave Acoustics*), vol. 13, Mar. 1970.
[3] J. H. Collins and P. J. Hagon, "Surface wave delay lines promise filters for radar, flat tubes for television and fasten computers," *Electronics*, vol. 43, Jan. 1970.
[4] E. Stern, "Microwave components, circuits and applications," Lincoln Lab. Tech. Note 1968-36, Oct. 1968.
[5] L. R. Adkins, T. W. Bristol, P. J. Hagon, and A. J. Hughes, "Surface acoustic waves—Device applications and signal routing techniques for VHF and UHF," *Microwave J.*, vol. 13, Mar. 1970.
[6] W. R. Smith *et al.*, "Analysis of interdigital surface wave transducers by use of an equivalent circuit model," *IEEE Trans. Microwave Theory Tech.* (*Special Issue on Microwave Acoustics*), vol. MTT-17, pp. 856–864, Nov. 1969.
[7] ——, "Design of surface wave delay lines with interdigital transducers," *IEEE Trans. Microwave Theory Tech.* (*Special Issue on Microwave Acoustics*), vol. MTT-17, pp. 865–873, Nov. 1969.
[8] A. P. Van Den Heurel, D. B. Owen, and S. G. Joshi, "Hybrid transducer: A new technique for generating surface waves on non-piezoelectric substrates," presented at the IEEE G-SU Ultrasonics Symp., St. Louis, Mo., Sept. 1969, Paper C-8.
[9] W. C. Wang, P. Staecker, and R. C. M. Li, "Elastic waves bound to a fluid layer between two adjacent solids," *Appl. Phys. Lett.*, vol. 16, Apr. 1970.
[10] R. C. M. Li and K. H. Yen, "Elastic waves guided by a solid layer between adjacent substrates," *IEEE Trans. Microwave Theory Tech.*, vol. MTT-20, pp. 477–486, July 1972.
[11] H. S. Tuan and C. P. Chang, "Tapping of Love waves in an isotropic surface waveguide by surface-to-bulk wave transduction," *IEEE Trans. Microwave Theory Tech.*, vol. MTT-20, pp. 472–477, July 1972.
[12] P. M. Morse and H. Feshback, *Methods of Theoretical Physics*, vol. 2. New York: McGraw-Hill, 1953, ch. 9.
[13] Y. M. Chen and S. J. Kim, "Scattering of acoustic waves by a penetrable sphere with statistically corrugated surface," *J. Acoust. Soc. Amer.*, vol. 42, July 1967.
[14] R. E. Collin, *Field Theory of Guided Waves.* New York: McGraw-Hill, 1960, ch. 11.
[15] I. Abubakar, "Scattering of plane elastic waves at rough surfaces I, II," *Proc. Cambridge Phil. Soc.*, vol. 58 and 59, 1962.
[16] B. A. Auld, "Application of microwave concepts to the theory of acoustic fields and waves in solids," *IEEE Trans. Microwave Theory Tech.* (*Special Issue on Microwave Acoustics*), vol. MTT-17, pp. 800–811, Nov. 1969.

Coupling Errors in Cavity-Resonance Measurements on MIC Dielectrics

P. H. LADBROOKE, M. H. N. POTOK, AND E. H. ENGLAND

***Abstract*—Measurements on MIC dielectrics have been made by applying the theory of resonant cavities to either wholly or partly metallized substrates. Two different schemes of coupling are employed, depending upon the metallization. Errors occur in the derived value of ϵ, due to the coupling, and are of opposite sense for the two methods discussed. They may be averaged to improve the overall measurement precision (0.5 percent).**

Several authors have recently described a convenient way of measuring the permittivity of MIC substrate materials [1], [2], [6]. The substrate, which may typically be 2.5 cm square by 0.5 mm thick for Al_2O_3 (alumina and sapphire) and 1.5–2 times larger for quartz, is simply metallized on some or all of its faces, and cavity resonances are excited in it from which ϵ may be deduced. We have used both completely and partly metallized cavities to measure ϵ for 15 samples of Al_2O_3 and find a scatter of a few percent in the experimental data which is related to the perturbation of the cavity fields at the coupling points, the coupling method being different for the two different metallization schemes. These two methods lead to errors of opposite sense, and hence yield a more accurate averaged value for ϵ than if either set were used alone. Of more immediate interest to the practicing engineer is the finding that certain specific resonances require no correction at all, yielding quick and accurate answers.

The basic structures investigated are shown in Fig. 1. In Fig. 1(a), the two large faces are metallized, but the sidewalls are left uncoated [1]. Excitation and detection are effected at the corners using the HP 8410A/8740A network analyzer system [1]. We refer to such cavities as having open-circuit or magnetic sidewalls. For Fig. 1(b), the substrate is metallized all over, and two apertures are photolithographically cut: one for excitation via an overlaid stripline 3 mm in diameter at $(y_1/5, z_1/5)$ in the broad face and the other (smaller) 1 mm long in a sidewall for detection via a loop probe. This device we refer to as having short-circuit or electric sidewalls.

In trying to establish a philosophy for coupling with coated edges, we first of all tried cutting two apertures in the sidewalls; however, with this arrangement, only a few of the modes possible could be found—mainly due to there being no probe penetration into the solid dielectric. A broadwall hole with overlaid stripline provides tighter

Manuscript received November 30, 1972, revised February 15, 1973.
The authors are with the Department of Electrical and Electronic Engineering, Royal Military College of Science, Shrivenham, Swindon, Wilts., England.